Theoretical insights into hybrid perovskites for photovoltaic applications

Jacky Even, Soline Boyer-Richard, Marcelo Carignano, Laurent Pedesseau, Jean-Marc Jancu, Claudine Katan

Theoretical insights into hybrid perovskites for photovoltaic applications

Jacky Even*[a], Soline Boyer-Richard[a], Marcelo Carignano[b], Laurent Pedesseau[a], Jean-Marc Jancu[a], Claudine Katan[c]

[a]Université Européenne de Bretagne, INSA, FOTON UMR 6082, 35708 Rennes, France;
[b]Qatar Environment and Energy Research Institute, Hamad Bin Khalifa University, Doha, Qatar
[c]Institut des Sciences Chimiques de Rennes, UMR 6226, CNRS – Université de Rennes 1, France;

ABSTRACT

In this paper, we examine recent theoretical investigations on 3D hybrid perovskites (HOP) that combine concepts developed for classical bulk solid-state physics and empirical simulations of their optoelectronic properties. In fact, the complexity of HOP calls for a coherent global view that combines usually disconnected concepts. For the pseudocubic high temperature reference perovskite structure that plays a central role for 3D HOP, we introduce a new tight-binding Hamiltonian, which specifically includes spin-orbit coupling. The resultant electronic band structure is compared to that obtained using state of the art density functional theory (DFT). Next, recent experimental investigations of excitonic properties in HOP will be revisited within the scope of theoretical concepts already well implemented in the field of conventional semiconductors. Last, possible plastic crystal and orientational glass behaviors of HOP will be discussed, building on Car-Parrinello molecular dynamics simulations.

Keywords: hybrid perovskite, tight binding, band structure, optical absorption, exciton, molecular dynamics, plastic crystal, orientational glass

1. INTRODUCTION

In the last few years, a scientific breakthrough for solar cells occurred with 3D Hybrid Organic Perovskites (HOP) of general the chemical formulae $MABX_3$, where MA is an organic cation $CH_3NH_3^+$, X is a halogen atom (X=I, Br, Cl) and B a metal atom (B=Pb, Sn). The efficiency of hybrid perovskites solar cells rose rapidly from 3.8% in 2009 with DSSC-like technologies to about 10% in 2012 using new concepts [1][2][3][4]. These record values steeply increased to about 15% in 2013 thanks to new deposition techniques[5][6]. At the end of 2014, optimized conversion efficiency amounts to 19.3% and then 21% in the last (January 2016) NREL efficiency chart [8]. In addition to the current certified world record, over 21% efficiency was announced for a perovskite on silicon tandem cell at the HOPV15 held in Rome May 2015. Clearly, in the midst of such a rise, understanding physical properties of operational HOP and design of novel devices with improved performances is important and can greatly benefit from theoretical approaches. Prior to 2013, most theoretical studies either focused on layered HOP [8] or purely inorganic 3D perovskites, and the few dealing with 3D HOP manifestly neglected inherent physical properties such as the spin-orbit coupling (SOC). In 2013, a few theoretical papers started to appear on 3D HOP following their breakthrough in the field of photovoltaics, currently resulting in an exponential growth [9][10][11][12]. Since the initial outbreak, significant progress has been made towards the understanding of the unusual physical properties of this new class of semiconductors [13][14]. In this work we design a novel tight-binding model and illustrate how it can accurately model the properties of HOP using the prototype $MAPbI_3$ material. Next, based on concepts and tools already well developed in the field of conventional semiconductors, we discuss nonlinear absorption and excitonic effects. Last, we determine whether and to what extent HOP may have plastic crystal phases or behave similarly to orientational glasses.

2. TIGHT BINDING METHOD AND RESULTS

The semi-empirical tight-binding method is a powerful formalism to describe the electronic structure in molecules and solids. Slater and Koster called it the tight binding or Bloch method and their historic paper in 1954 [15] “Simplified LCAO-method for the Periodic Potential Problems” gave a systematic procedure to build an orbital-based Hamiltonian in a multi-center approach within an interpolation scheme. Some methods include orbital overlap both in parameterizing

*jacky.even@insa-rennes.fr

citation: Jacky Even ; Soline Boyer-Richard ; Marcelo Carignano ; Laurent Pedesseau ; Jean-Marc Jancu, Claudine Katan " Theoretical insights into hybrid perovskites for photovoltaic applications ", *Proc. SPIE* 9742, Physics and Simulation of Optoelectronic Devices XXIV, 97421A (March 4, 2016); doi:10.1117/12.2213135; http://dx.doi.org/10.1117/12.2213135

the Hamiltonian and in the secular equation. In particular, the self-consistent charge density functional tight-binding which allows treating a large range of systems (clusters, biomolecules, hybrid nanostructures) with DFT accuracy [16]. Conversely, methods that neglect overlaps in the secular equation are usually labeled orthogonal and over the last 30 years there have been numerous applications which have been pursued in a variety of material problems, following different philosophies and placing different levels of emphasis on the required level of accuracy [17]. In this context, for

semiconductors, the extended-basis extended sp3d5s∗ tight binding model relies on the availability of correct approximations [18] and the unique ability to describe with the same precision any region of the Brillouin zone. It has been effective in accurately calculating physical properties of different structure configurations, for instance, in multi-million atom electronic structure simulations [19][20]. New developments of orthogonal models concern the exact representation of the local wave-function in real space suited to many-body calculations [21][22].

.

In this paper we use this approach to investigate the properties of HOP, considering the reference cubic structures of the 3D ABX_3 family. We underline that M. Kim and co-workers already proposed a tight binding Hamiltonian, developed on an 8 functions basis with SOC, for ABX_3 halide perovskites to model Rashba effect [23]. In their Hamiltonian, the triple bands come from the *p* orbitals of the B-site atom, and the single band from the *s* orbital of B and *p* orbitals of the surrounding halogens. They clearly obtain evidence of strong Rashba effect, thus confirming the DFT previous results of some of us [24], but do not claim that their TB scheme affords the real band structure.

Our tight-binding model is based on a 16 functions basis without SOC or a 32 functions basis with SOC. For cubic ABX_3 halide perovskites, we consider one "*s*" and three "*p*" orbitals for the B atom, and the same for each of the three X atoms in the simple cubic unit cell. No basis function is taken into account for the A organic molecule, which's position is not fixed because it has rotational degrees of freedom/disorder in the cubic phase. We only consider first neighbor interactions, only between B and X atoms. We have chosen the minimal sp^3 basis as developed by Slater and Koster and we have tried to reproduce the already known experimental data like energy band-gap and effective masses around the bandgap with our semi-empirical TB model. Nine parameters are considered without SOC: four different diagonal matrix elements related to the atomic energies of the chemical constituents B and X: E_{sB}, E_{pB}, E_{sX} and E_{pX}. Five transfer matrix elements refer to the overlap integral of atomic functions: V_{ss}, V_{sBpX}, V_{sXpB}, $V_{pp\sigma}$, $V_{pp\pi}$. SOC only appears for *p* orbitals with two SOC values Δ_{soB} and Δ_{soX}. The 32-band Hamiltonian is larger than the one obtained by Kim [11] but remains very empty. This method has been applied to $MaPbI_3$ cubic phase.

$MaPbI_3$ dispersion relation has been calculated using the sp^3 tight binding method including SOC. Figure 1 presents the band diagram obtained, fitting existing experimental and theoretical results [5][6][25]. The bandgap is obtained at R point with E_G = 1.620 eV. Effective masses around the bandgap are the following: $m_h^* = 0.235\, m_0$ and $m_e^* = 0.229\, m_0$. The dispersion relation shape is in very good agreement with the one obtained using DFT and many-body calculation [25].

citation: Jacky Even ; Soline Boyer-Richard ; Marcelo Carignano ; Laurent Pedesseau ; Jean-Marc Jancu, Claudine Katan " Theoretical insights into hybrid perovskites for photovoltaic applications ", *Proc. SPIE* 9742, Physics and Simulation of Optoelectronic Devices XXIV, 97421A (March 4, 2016); doi:10.1117/12.2213135; http://dx.doi.org/10.1117/12.2213135

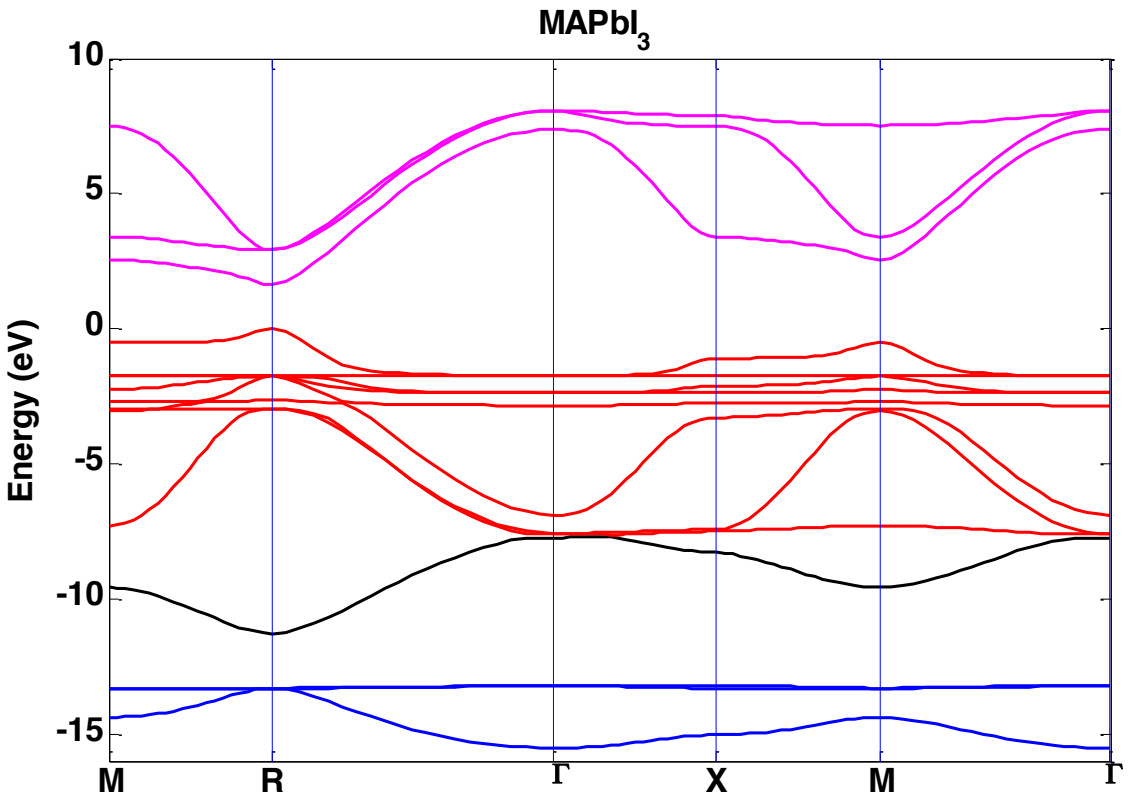

Figure 1. $MAPbI_3$ band diagram obtained within the TB scheme with SOC. The energy of valence band maximum is set to zero. Bands are colored according to their main orbital character: red depicts I *5p*, pink depicts Pb *6p*, black depicts Pb *6s* and blue depicts I *5s*. Points denoted M, X and R are zone-boundary points close to (1/2,1/2,0), (1/2,0,0) and (1/2,1/2,1/2) respectively. The Γ point is the BZ center.

Figure 2 shows the effect of spin-orbit coupling at R point around the energy bandgap in the conduction band. Without SOC, the energy bandgap value is 2.58 eV and the three Pb *6p* states are degenerated at R in the conduction band. SOC lifts this degeneracy. Six Pb states are now to be considered: the four Pb upper states are obtained at 2.91 eV and the two lower states are at 1.62 eV with a SOC value of $\Delta_{soB} = 1.3$ eV in the conduction band. In fact, in $MAPbI_3$ Δ_{soB} has been shown to be comparable to the bandgap energy ($E_G = 1.6$ eV) [13]. Another SOC is taken into account for I *p*-type states in the valence band: $\Delta_{soX} = 1.2$ eV. This SOC for halogen states has no effect around the energy bandgap but it plays a great role for the lower valence band dispersion relation. These results confirm the importance of SOC for both the metal and the halide predicted earlier [10][26].

citation: Jacky Even ; Soline Boyer-Richard ; Marcelo Carignano ; Laurent Pedesseau ; Jean-Marc Jancu, Claudine Katan " Theoretical insights into hybrid perovskites for photovoltaic applications ", *Proc. SPIE* 9742, Physics and Simulation of Optoelectronic Devices XXIV, 97421A (March 4, 2016); doi:10.1117/12.2213135; http://dx.doi.org/10.1117/12.2213135

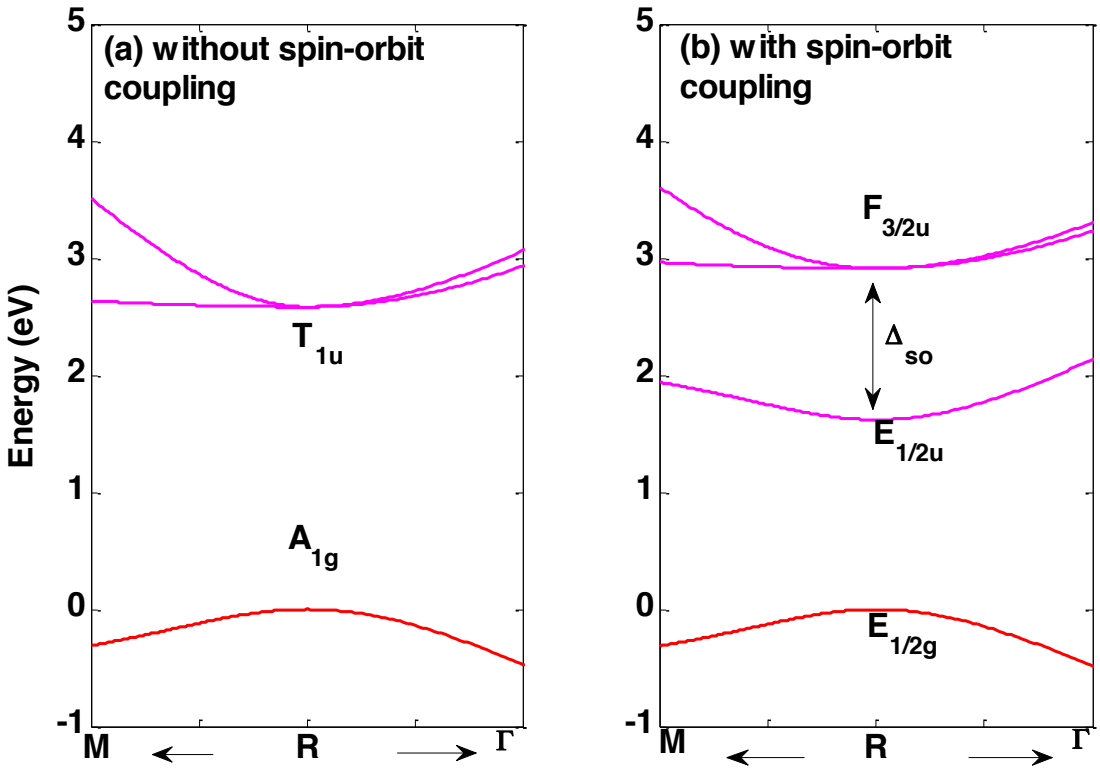

Figure 2: Effect of spin-orbit coupling in the conduction band near the R point. The energy of valence band maximum is set to zero. The arrows towards M and Γ denote the directions in reciprocal space. These band diagram zooms only represent 20% of the BZ in each direction. Labels of irreducible representation obtained for simple (a) or double (b) group representation are given at the R point near the bandgap. (a) Band diagram computed without SOC, (b) Band diagram computed with SOC: Δ_{so} = 1.3 eV.

As for the Γ point, R corresponds to a special high symmetry **k**-point for which the group of the wave vector is O_h. Without SOC, simple group irreducible representation (IR) is used. T_{1u} is the relevant IR for the bottom of the conduction band (equivalent to R_4^- in the P_{m3m} space group), and A_{1g} corresponds to the totally symmetric orbitals of the top of the valence band (equivalent to R_1^+ in the P_{m3m} space group). Considering SOC requires double groups: $E_{1/2g}$ is the electron spin IR: double space representations are deduced from the product of $E_{1/2g}$ with the simple group IR. Top valence band R-point IR is therefore $E_{1/2g}$. Conduction band minimum becomes a two-fold spin orbit-split off state named $E_{1/2u}$ (equivalent to R_6^- in P_{m3m} space group) and the remaining four-fold degenerated states is labelled $F_{3/2u}$ (equivalent to R_8^- in the P_{m3m} space group). A complete study of these symmetry properties is available in Ref. [13][26].

3. NON-LINEAR ABSORPTION AND EXCITONIC EFFECTS

Excitonic effects in semiconductor crystals can be accounted for using the Bethe-Salpeter Equation (BSE) starting from the monoelectronic states calculated at the DFT level, or even including many-body corrections at the DFT+GW level. When taking the pseudo-cubic high temperature reference phases of $MAPbI_3$, enhancement of absorption at the bandgap was clearly evidenced in the first DFT-based BSE simulations reported in the literature [24]. This simulation was in agreement with old experimental absorption spectra reporting a large exciton binding energy at 4K (~50meV). A careful reexamination of old experimental absorption spectra of $MAPbI_3$ at higher temperatures, from about 75K to the room

citation: Jacky Even ; Soline Boyer-Richard ; Marcelo Carignano ; Laurent Pedesseau ; Jean-Marc Jancu, Claudine Katan " Theoretical insights into hybrid perovskites for photovoltaic applications ", *Proc. SPIE* 9742, Physics and Simulation of Optoelectronic Devices XXIV, 97421A (March 4, 2016); doi:10.1117/12.2213135; http://dx.doi.org/10.1117/12.2213135

temperature revealed the importance of the exciton screening at high temperature. This interpretation was later on confirmed by detailed experimental observations. In fact, using a theoretical expression accounting both for bound pair states and a continuum of pair states to simulate the optical absorption clearly showed that the generally accepted value of the dielectric constant for $MAPbI_3$ is inappropriate for describing the real exciton resonance at room temperature. In the perturbative BSE/DFT or BSE/DFT+GW approach, screening of the electron-hole interaction due to atomic motion or molecular fast rotations (vide infra) is however not taken into account, and is more suited to the low temperature phases where these motions are frozen.

The modifications of exciton resonances by a change of the dielectric constant related to ionic contributions or free carriers may be simplified by combining an empirical method for the monoelectronic eigenstates and the computation of the exciton Green's function. In order to account for non-linear effects induced by a free carrier population, a full BSE/DFT or BSE/DFT+GW treatment is indeed beyond available computational resources. The optical susceptibility can be written in terms of the exciton Green's function and the BSE is used to compute the exciton Green's function. In this work, we use an empirical basis of electron and hole monoelectronic states obtained with the k.p method, to analyse the modifications of the optical spectrum close to the band gap [28]. In the linear regime, the BSE contains the dipole of the e-h optical transition at R as a source term for the Green function and an e-h Coulomb interaction, which singularity deserves a specific numerical procedure. Figure 3 is the result of the computation of the optical absorption spectrum assuming a small dielectric constant (6.5), therefore adapted to the exciton at low temperature in the linear regime. The simulation shows a strong 1S exciton resonance, together with additional 2S, 3S resonances and low continuum optical absorption above the electronic band gap.

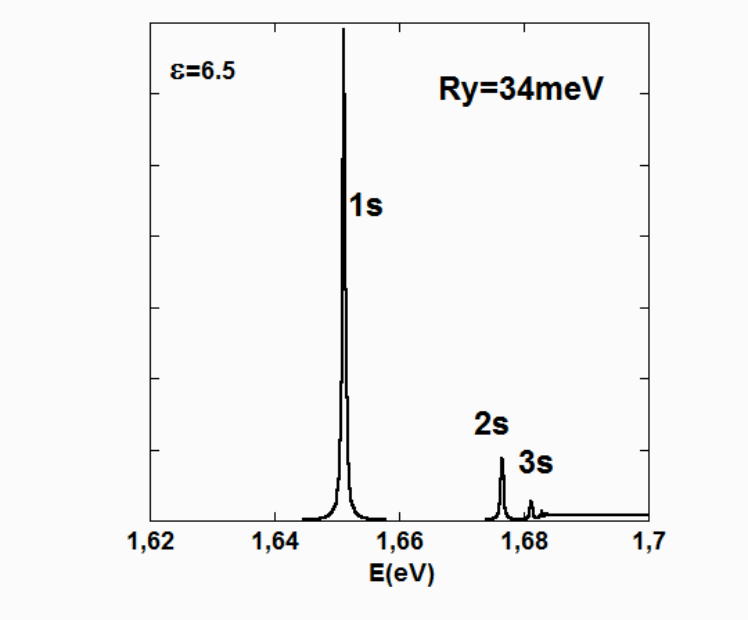

Figure 3: The optical absorption of $MAPbI_3$ computed using the BSE and the exciton Green's function in the linear regime at low temperature. An empirical basis of electron and hole monoelectronic states obtained with the **k.p** method close to the R point is used to compute the exciton Green's function. The e-h Coulomb interaction is computed with an effective dielectric constant equal to 6.5. 1s-3s exciton resonances are shown (the electronic band gap is set at 1.685eV)

In the non-linear regime and under the influence of a plasma of free carriers, the BSE equation is strongly modified: *1)* the e-h Coulomb interaction is screened, which is usually represented within the plasmon-pole approximation, *2)* the oscillator strength is reduced by the phase-space population due to free carriers, and *3)* self-energy contributions for both electrons and holes, lead to band gap renormalization and damping of the exciton resonances (figure 4).

citation: Jacky Even ; Soline Boyer-Richard ; Marcelo Carignano ; Laurent Pedesseau ; Jean-Marc Jancu, Claudine Katan " Theoretical insights into hybrid perovskites for photovoltaic applications ", *Proc. SPIE* 9742, Physics and Simulation of Optoelectronic Devices XXIV, 97421A (March 4, 2016); doi:10.1117/12.2213135; http://dx.doi.org/10.1117/12.2213135

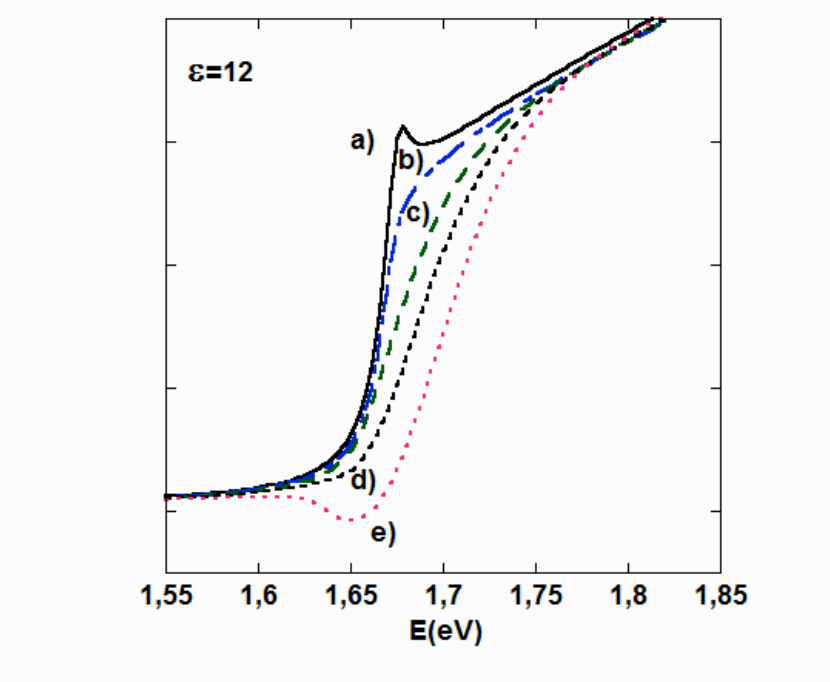

Figure 4: Optical absorption of $MAPbI_3$ computed using the BSE and the exciton Green's function in the non-linear regime at T=160K. The concentration of free carriers is equal to: a) 0, b) $10^{17}cm^{-3}$, c) $5.10^{17}cm^{-3}$, d) $10^{18}cm^{-3}$, e) $2.10^{18}cm^{-3}$. The band gap in the linear regime is set to 1.685eV

Figure 4 is the result of the computation of the optical absorption spectrum assuming an intermediate dielectric constant (12), adapted to the exciton at about T=160K where the exciton binding energy is reduced [13]. For moderate free carrier concentrations of about $10^{17}cm^{-3}$, the screening of the exciton resonance is the most important phenomenon. For larger concentrations $5.10^{17}cm^{-3}/10^{18}$cm-3, phase space filling effects start to dominate until population inversion is reached for $2.10^{18}cm^{-3}$. For low carrier concentrations, the band gap renormalization is partially compensated by the screening of the exciton resonance. For large concentration the band gap is shifted to lower values (about 1.65eV for $2.10^{18}cm^{-3}$).

4. PLASTIC CRYSTAL PHASE AND ORIENTIONAL GLASS BEHAVIOR

$MAPbI_3$ and $MAPbBr_3$ crystals exhibit low temperature Pnma orthorhombic phases, where the molecular orientations are fixed. Fast MA cation reorientations occur in the cubic (Pm3m) and tetragonal (I4/mcm) high temperature phases. The characteristics of this motion, namely existence of stochastic orientational degrees of freedom at high temperature [29], can be assessed from experimental results reported in the literature. Recent quasi-elastic incoherent neutron scattering results, recorded on $MAPbI_3$ or $MAPbBr_3$ powders, are consistent with the simultaneous fast rotations of the methyl and ammonium groups around the C-N axes and the slower tumbling of the C-N axis between symmetry equivalent position [31][32][29]. This is described with a C_4xC_3 symmetry-based jump model designed for the tetragonal phase [31]. The existence of a stochastic reorientational motion, leading to a collective freezing at low temperature and thus a plastic crystal behavior, has been thoroughly analyzed in [29], combining group theory analysis and the concepts of discrete molecular pseudospins and continuous rotator functions. Additional first principles molecular dynamics simulations were performed using the CP2K package under NVT ensemble using periodic boundary conditions with the temperature controlled using a Nosé-Hoover thermostat. The electronic structure properties were calculated using the PBE functional with the addition of the Grimme D3 scheme to correct dispersion interactions. The time-step for the integration of the dynamic equation was set to 1 fs. Figure 5 represents the average autocorrelation function of the CN axis orientation in $MAPbI_3$ extracted from MD simulations performed on a 444 cubic supercell. These molecular dynamics simulations clearly show a slowing down of the critical reorientational fluctuations as a function of the temperature (Figure 5).

citation: Jacky Even ; Soline Boyer-Richard ; Marcelo Carignano ; Laurent Pedesseau ; Jean-Marc Jancu, Claudine Katan " Theoretical insights into hybrid perovskites for photovoltaic applications ", *Proc. SPIE* 9742, Physics and Simulation of Optoelectronic Devices XXIV, 97421A (March 4, 2016); doi:10.1117/12.2213135; http://dx.doi.org/10.1117/12.2213135

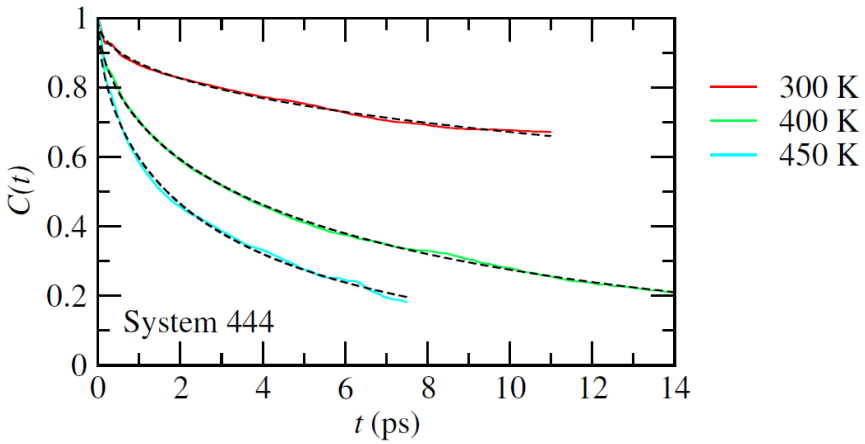

Figure 5: Temperature dependence of the average autocorrelation function of the CN axis orientation in $MAPbI_3$ extracted from first principles MD simulations for a 444 cubic supercell (solid lines): (top) 300K, (middle) 400K and (bottom) 450K. Dashed lines are fits using stretched exponential functions.

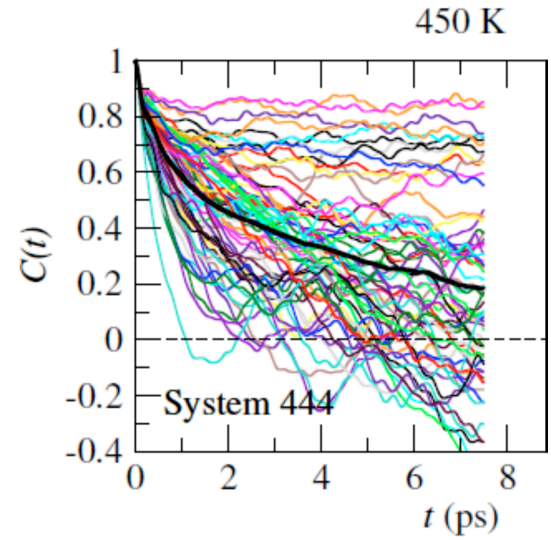

Figure 6: Time dependence of the autocorrelation function for all molecules within the 444 supercell extracted from first principles MD simulation at T=450K. The average time dependence is plotted in bold dark for comparison.

When typical plastic crystals are cooled, the rotational motion freezes and, an orientational order appears at low temperature. Plastic crystals may exhibit two different behaviors in this temperature range. In the first case, the rotational motion freezes under careful cooling, keeping quasistatic random molecular orientations. These materials are orientational glasses, which exhibit most of the properties related to conventional glasses, such as specific heat anomalies, ageing and distributions of relaxation times. Prototypes of orientational glasses are cyclohexanol and cyanoadamantane. In the second case, spatial correlations or interactions between molecular orientations are strong. The plastic crystal undergoes a structural transition at low temperature to a partially or completely ordered crystalline phase. Molecular dynamics studies have revealed through the study of the molecular orientational distribution, that the intermolecular correlations are weak [29]. Moreover, recent neutron scattering experiments have also revealed that only a minor fraction of the MA cations is involved in rotational motions in the high temperature phases (T>160K for $MAPbI_3$) [30]. This is also consistent with our MD simulations (Figure 6) [29]. In fact, the time dependence of the average autocorrelation function for molecular reorientation in the MD is strongly non-exponential (Figure 5) and can be

citation: Jacky Even ; Soline Boyer-Richard ; Marcelo Carignano ; Laurent Pedesseau ; Jean-Marc Jancu, Claudine Katan " Theoretical insights into hybrid perovskites for photovoltaic applications ", *Proc. SPIE* 9742, Physics and Simulation of Optoelectronic Devices XXIV, 97421A (March 4, 2016); doi:10.1117/12.2213135; http://dx.doi.org/10.1117/12.2213135

nicely fitted using stretched exponentials. Detailed inspection of the dynamics at T=450K (Figure 6) reveals that it is related to a wide dispersion of reorientational dynamics of individual molecules. This might be indicative of remaining static disorder in the orientations of the cations at very low temperature, thus to an incomplete long range freezing of cation's orientations: in other words, an orientational glass. A significant part of the cations (roughly 30%) remain almost frozen with respect to a tumbling motion on the time scale of our MD trajectory [29]. At low temperature, frustrated interactions are expected to lead to an orientational glass behavior where translational symmetry is broken for the molecular orientations [29]. This prediction was confirmed experimentally very recently [33], showing dielectric and calorimetric signatures typical of glassy states.

5. CONCLUSION

This review shows that combining various sophisticated theoretical approaches is useful to study the optoelectronic properties of HOP compounds. A new atomistic empirical method is proposed to describe the electronic properties of HOP, including spin-orbit coupling effects. This method is promising for future simulations of large scale HOP nanostructures. Moreover, it is shown that the solution of the BSE equation may start from an empirical basis of electron and hole monoelectronic states obtained with the k.p method close to the critical R point. The computation of the exciton Green's function including interaction with a free carrier gas is then possible, leading to a description of exciton screening, band gap renormalisation and population inversion effects. Finally, a new approach for the stochastic rotational motions of the cations in HOP leads to the definition of symmetry-based molecular pseudospins and rotator functions. The high temperature reference cubic phase of HOP is described as a plastic crystal, and an orientational glass behavior is predicted at low temperature, in agreement with recent dielectric and thermodynamic characterizations.

6. ACKNOWLEDGEMENTS

This project has received funding from the European Union's Horizon 2020 research and innovation Program under the grant agreement No 687008 (GOTSolar). The work at FOTON is supported by Agence Nationale pour la Recherche (Snap and Supersansplomb projects) and was performed using HPC resources from GENCI-CINES/IDRIS grant 2016-c2012096724. J. E. work is supported by the Fondation d'entreprises banque Populaire de l'Ouest under Grant PEROPHOT 2015.

REFERENCES

[1] Kojima, A., Teshima, K., Shirai, Y. and Miyasaka, T., "Organometal Halide Perovskites as Visible-Light Sensitizers for Photovoltaic Cells," J. Am. Chem. Soc. 131 (17), 6050-6051 (2009).
[2] Im, J. H., Lee, C. R., Lee, J. W., Park, S. W. and Park, N. G., "6.5% Efficient Perovskite Quantum-Dot-Sensitized Solar Cell." Nanoscale, 3(10), 4088−4093 (2011).
[3] Lee, M. M., Teuscher, J., Miyasaka, T., Murakami, T. N. and Snaith, H. J., "Efficient Hybrid Solar Cells Based on Meso-Superstructured Organometal Halide Perovskites," Science 338, 643-647 (2012).
[4] Kim, H. S., Lee, C. R., Im, J. H., Lee, K. B., Moehl, T., Marchioro, A., Moon, S. J., Humphry-Baker, R., Yum, J. H., Moser, J. E., Grätzel, M. and Park, N-G., "Lead Iodide Perovskite Sensitized All-Solid-State Submicron Thin Film Mesoscopic Solar Cell with Efficiency Exceeding 9%," Sci. Rep. 2, 591-591-7 (2012).
[5] Burschka, J., Pellet, N., Moon, S. J., Humphry-Baker, R., Gao, P., Nazeeruddin, M.K. and Grätzel, M., "Sequential deposition as a route to high-performance perovskite-sensitized solar cells," Nature 499, 316–319 (2013).
[6] Liu, M., Johnston, M. B. and Snaith, H. J., "Efficient planar heterojunction perovskite solar cells by vapour deposition," Nature 501, 395-398 (2013).

citation: Jacky Even ; Soline Boyer-Richard ; Marcelo Carignano ; Laurent Pedesseau ; Jean-Marc Jancu, Claudine Katan " Theoretical insights into hybrid perovskites for photovoltaic applications ", *Proc. SPIE* 9742, Physics and Simulation of Optoelectronic Devices XXIV, 97421A (March 4, 2016); doi:10.1117/12.2213135; http://dx.doi.org/10.1117/12.2213135

[7] http://www.nrel.gov/ncpv/images/efficiency_chart.jpg
[8] Even, J., Pedesseau, L., Dupertuis, M.-A., Jancu, J.-M. and Katan, C., "Electronic model for self-assembled hybrid organic/perovskite semiconductors: Reverse band edge electronic states ordering and spin-orbit coupling," Phys. Rev. B. 86, 205301-1-205301-4 (2012).
[9] Mosconi, E., Amat, A., Nazeeruddin, Md. K., Grätzel, M., De Angelis, F., "First-principles modeling of mixed halide organometal perovskites for photovoltaic applications," J. Phys. Chem. C, 117, 13902-13913 (2013).
[10] Even, J., Pedesseau, L., Jancu, J.-M. and Katan, C., "Importance of spin–orbit coupling in hybrid organic/inorganic perovskites for photovoltaic applications," J. Phys. Chem. Lett. 4, 2999-3005 (2013).
[11] Brivio, F., Walker, A. B., Walsh, A, "Structural and electronic properties of hybrid perovskites for high-efficiency thin-film photovoltaics from first-principles," Appl. Phys. Lett. Mat. 1, 042111-1-042111-5 (2013).
[12] Giorgi, V., Fujisawa, J.-I., Segawa, H., Yamashita, K., "Small photocarrier effective masses featuring ambipolar transport in methylammonium lead iodide perovskite: A density functional analysis," J. Phys. Chem. Lett. 4, 4213-4216 (2013).
[13] Even, J., Pedesseau, L. and Katan, C., "Analysis of multivalley and multibandgap absorption and enhancement of free carriers related to exciton screening in hybrid perovskites," J. Phys. Chem. C 118, 11566-11572 (2014).
[14] Even, J., Pedesseau, L., Katan, C., Kepenekian, M., Lauret, J.-S., Sapori, D., and Deleporte, E., "Solid-State Physics Perspective on Hybrid Perovskite Semiconductors," J. Phys. Chem. C. 119, 10161-10177 (2015).
[15] Slater, J. C. & Koster, G. F. "Simplified LCAO method for the periodic potential problem." Phys. Rev. 94, 1498–1524 (1954).
[16] Elstner, M.; Seifert, G. "Density functional tight binding". Phil. Trans. R. Soc. A, 372, 20120483 (2014)
[17] Harrison W. A., "Electronic Structure and Properties of Solids," Freeman and Compagny, San Francisco, (1980).
[18] Jancu, J., Scholz, R., Beltram, F. & Bassani, F. "Empirical spds * tight-binding calculation for cubic semiconductors : General method and material parameters." Phys. Rev. B 57, 6493 (1998).
[19] Klimeck, G., Oyafuso, F., Boykin, T. B., Bowen, R. C. & von Allmen, P. "Development of a nanoelectronic 3D (NEMO 3D) simulator for multimillion atom simulations and its application to alloyed quantum dots." Comput. Model. Eng. Sci. 3, 601–642 (2002).
[20] Robert, C. et al. "Strain-induced fundamental optical transition in (In,Ga)As/GaP quantum dots." Appl. Phys. Lett. 104, 011908 (2014).
[21] Benchamekh, R. et al. "Tight-binding calculations of image-charge effects in colloidal nanoscale platelets of CdSe." Phys. Rev. B 89, 35307 (2014).
[22] Benchamekh, R. et al. "Microscopic electronic wave function and interactions between quasiparticles in empirical tight-binding theory". Phys. Rev. B 91, 45118 (2015).
[23] Kim, M., Im, J., Freeman, A. J., Ihm, J. & Jin, H. "Switchable S = 1/2 and J = 1/2 Rashba bands in ferroelectric halide perovskites." Proc. Natl. Acad. Sci. 111, 6900–6904 (2014).
[24] Even, J., Pedesseau, L., Jancu, J.-M. and Katan, C., "DFT and k • p modelling of the phase transitions of lead and tin halide perovskites for photovoltaic cells," Phys. Status Solidi RRL. 8, 31–35 (2014).
[25] Brivio, F., Butler, K. T., Walsh, A. & Van Schilfgaarde, M. "Relativistic quasiparticle self-consistent electronic structure of hybrid halide perovskite photovoltaic absorbers." Phys. Rev. B 89, 1–6 (2014).
[26] Katan, C., Pedesseau, L., Kepenekian, M., Rolland, A. & Even, J. "Interplay of spin–orbit coupling and lattice distortion in metal substituted 3D tri-chloride hybrid perovskites." J. Mater. Chem. A, 3, 9232-9240 (2015).
[27] Even, J. "Pedestrian Guide to Symmetry Properties of the Reference Cubic Structure of 3D All-Inorganic and Hybrid Perovskites." J. Phys. Chem. Lett. 6, 2238–2242 (2015).
[28] Haug, H. & Koch, S. W. "Quantum Theory of the Optical and Electronic Properties of Semiconductors." World Scientific, Singapore, (1990).
[29] Even, J., Carignano, M. & Katan, C. "Molecular disorder and translation/rotation coupling in the plastic crystal phase of hybrid perovskites." Nanoscale DOI: 10.1039/C5NR06386H, (2016)
[30] Leguy, A. M. A. , Frost, J.M., McMahon, A.P., Sakai, V.G., Kochelmann, W., Law, C.H., Li, X., Foglia, F., Walsh,A., O'Regan, B.C., Nelson, J., Cabral, J.T. & Barnes, P.R.F. "The dynamics of methylammonium ions in hybrid organic–inorganic perovskite solar cells." Nat. Commun., 6, 7124 (2015).
[31] Chen, T., Foley, B.J., Ipek, B., Tyagi, M., Copley, J. R. D., Brown, C.M., Choi, J.J. & Lee, S. "Rotational dynamics of organic cations in the CH3NH3PbI3 perovskite." Phys. Chem. Chem. Phys., 17, 31278-31286 (2015).
[32] Swainson, I.P., Stock, C., Parker, S.F., Van Eijck, L., Russina, M. & Taylor, J.W. "From soft harmonic phonons to fast relaxational dynamics in CH3NH3PbBr3." Phys. Rev. B, 92, 100303(R) (2015).

citation: Jacky Even ; Soline Boyer-Richard ; Marcelo Carignano ; Laurent Pedesseau ; Jean-Marc Jancu, Claudine Katan " Theoretical insights into hybrid perovskites for photovoltaic applications ", *Proc. SPIE* 9742, Physics and Simulation of Optoelectronic Devices XXIV, 97421A (March 4, 2016); doi:10.1117/12.2213135; http://dx.doi.org/10.1117/12.2213135

[33] Fabini, D.H., Hogan, T., Evans, H. A., Stoumpos, C.C., Kanatzidis, M.G. & Seshadri, R. “Dielectric and thermodynamic signatures of low-temperature glassy dynamics in the hybrid perovskites CH3NH3PbI3 and HC(NH2)2PbI3.” J. Phys. Chem. Lett. 7, 376-381 (2016)

citation: Jacky Even ; Soline Boyer-Richard ; Marcelo Carignano ; Laurent Pedesseau ; Jean-Marc Jancu, Claudine Katan " Theoretical insights into hybrid perovskites for photovoltaic applications ", *Proc. SPIE* 9742, Physics and Simulation of Optoelectronic Devices XXIV, 97421A (March 4, 2016); doi:10.1117/12.2213135; http://dx.doi.org/10.1117/12.2213135